

Graphene decorated microfiber for ultrafast optical modulation

Shaoliang Yu,¹ Chao Meng,¹ Bigeng Chen,¹ Hongqing Wang,² Xiaoqin Wu,¹ Weitao Liu,² Shangjian Zhang,³ Yong Liu,³ Yikai Su,⁴ and Limin Tong^{1,*}

¹State Key Laboratory of Modern Optical Instrumentation, Department of Optical Engineering, Zhejiang University, Hangzhou 310027, China

²Department of Physics, State Key Laboratory of Surface Physics, Laboratory of Advanced Materials and Key Laboratory of Micro and Nano Photonic Structures (Ministry of Education), Fudan University, Shanghai 200433, China

³State Key Laboratory on Electronic Thin Film and Integrated Devices, School of Optoelectronic Information, University of Electronic Science and Technology of China, Chengdu 610054, China

⁴State Key Laboratory of Advanced Optical Communication Systems and Networks, Department of Electronic Engineering, Shanghai Jiao Tong University, Shanghai 200240, China

*phytong@zju.edu.cn

Abstract: We demonstrate ultrafast optical modulation using a single 1- μm -diameter graphene-decorated microfiber, which is fabricated with a convenient and controllable evanescent-field-induced deposition method. Benefitting from the significantly enhanced light-graphene interaction of the subwavelength transvers dimension of the microfiber and accumulation of the saturable absorption of the piled graphene flakes, the microfiber shows nonlinear saturable absorption with a peak power threshold down to 1.75 W (60 MW/cm²), with a measured response time of about 3.5 ps.

©2015 Optical Society of America

OCIS codes: (230.4320) Nonlinear optical devices; (320.7085) Ultrafast information processing; (060.4080) Modulation.

References and links

1. F. Bonaccorso, Z. Sun, T. Hasan, and A. C. Ferrari, "Graphene photonics and optoelectronics," *Nat. Photonics* **4**(9), 611–622 (2010).
 2. Q. Bao and K. P. Loh, "Graphene photonics, plasmonics, and broadband optoelectronic devices," *ACS Nano* **6**(5), 3677–3694 (2012).
 3. K. S. Novoselov, V. I. Fal'ko, L. Colombo, P. R. Gellert, M. G. Schwab, and K. Kim, "A roadmap for graphene," *Nature* **490**(7419), 192–200 (2012).
 4. S. Yamashita, A. Martinez, and B. Xu, "Short pulse fiber lasers mode-locked by carbon nanotubes and graphene," *Opt. Fiber Technol.* **20**(6), 702–713 (2014).
 5. Q. L. Bao, H. Zhang, Y. Wang, Z. H. Ni, Y. L. Yan, Z. X. Shen, K. P. Loh, and D. Y. Tang, "Atomic-layer graphene as a saturable absorber for ultrafast pulsed lasers," *Adv. Funct. Mater.* **19**(19), 3077–3083 (2009).
 6. Z. Sun, T. Hasan, F. Torrisi, D. Popa, G. Privitera, F. Wang, F. Bonaccorso, D. M. Basko, and A. C. Ferrari, "Graphene mode-locked ultrafast laser," *ACS Nano* **4**(2), 803–810 (2010).
 7. M. Liu, X. Yin, E. Ulin-Avila, B. Geng, T. Zentgraf, L. Ju, F. Wang, and X. Zhang, "A graphene-based broadband optical modulator," *Nature* **474**(7349), 64–67 (2011).
 8. W. Li, B. Chen, C. Meng, W. Fang, Y. Xiao, X. Li, Z. Hu, Y. Xu, L. Tong, H. Wang, W. Liu, J. Bao, and Y. R. Shen, "Ultrafast all-optical graphene modulator," *Nano Lett.* **14**(2), 955–959 (2014).
 9. Z.-B. Liu, M. Feng, W.-S. Jiang, W. Xin, P. Wang, Q.-W. Sheng, Y.-G. Liu, D. N. Wang, W.-Y. Zhou, and J.-G. Tian, "Broadband all-optical modulation using a graphene-covered-microfiber," *Laser Phys. Lett.* **10**(6), 065901 (2013).
 10. Z. Sun and H. Chang, "Graphene and graphene-like two-dimensional materials in photodetection: mechanisms and methodology," *ACS Nano* **8**(5), 4133–4156 (2014).
 11. F. Xia, T. Mueller, Y. M. Lin, A. Valdes-Garcia, and P. Avouris, "Ultrafast graphene photodetector," *Nat. Nanotechnol.* **4**(12), 839–843 (2009).
 12. X. T. Gan, R. J. Shiue, Y. D. Gao, I. Meric, T. F. Heinz, K. Shepard, J. Hone, S. Assefa, and D. Englund, "Chip-integrated ultrafast graphene photodetector with high responsivity," *Nat. Photonics* **7**(11), 883–887 (2013).
 13. X. M. Wang, Z. Z. Cheng, K. Xu, H. K. Tsang, and J. B. Xu, "High-responsivity graphene/silicon-heterostructure waveguide photodetectors," *Nat. Photonics* **7**(11), 888–891 (2013).
 14. A. Pospischil, M. Humer, M. M. Furchi, D. Bachmann, R. Guider, T. Fromherz, and T. Mueller, "CMOS-compatible graphene photodetector covering all optical communication bands," *Nat. Photonics* **7**(11), 892–896 (2013).
-

15. J. M. Dawlaty, S. Shivaraman, M. Chandrashekhara, F. Rana, and M. G. Spencer, "Measurement of ultrafast carrier dynamics in epitaxial graphene," *Appl. Phys. Lett.* **92**(4), 042116 (2008).
16. S. J. Koester and M. Li, "Waveguide-coupled graphene optoelectronics," *IEEE J. Sel. Top. Quantum Electron.* **20**(1), 6000211 (2014).
17. B. Chen, C. Meng, Z. Yang, W. Li, S. Lin, T. Gu, X. Guo, D. Wang, S. Yu, C. W. Wong, and L. Tong, "Graphene coated ZnO nanowire optical waveguides," *Opt. Express* **22**(20), 24276–24285 (2014).
18. Y. Wu, B. Yao, A. Zhang, Y. Rao, Z. Wang, Y. Cheng, Y. Gong, W. Zhang, Y. Chen, and K. S. Chiang, "Graphene-coated microfiber Bragg grating for high-sensitivity gas sensing," *Opt. Lett.* **39**(5), 1235–1237 (2014).
19. K. Kashiwagi and S. Yamashita, "Deposition of carbon nanotubes around microfiber via evanescent light," *Opt. Express* **17**(20), 18364–18370 (2009).
20. J. Z. Wang, Z. Q. Luo, M. Zhou, C. C. Ye, H. Y. Fu, Z. P. Cai, H. H. Cheng, H. Y. Xu, and W. Qi, "Evanescent-light deposition of graphene onto tapered fibers for passive Q-switch and mode-locker," *IEEE Photonics J.* **4**(5), 1295–1305 (2012).
21. N. Zhao, M. Liu, H. Liu, X. W. Zheng, Q. Y. Ning, A. P. Luo, Z. C. Luo, and W. C. Xu, "Dual-wavelength rectangular pulse Yb-doped fiber laser using a microfiber-based graphene saturable absorber," *Opt. Express* **22**(9), 10906–10913 (2014).
22. L. Tong, J. Lou, and E. Mazur, "Single-mode guiding properties of subwavelength-diameter silica and silicon wire waveguides," *Opt. Express* **12**(6), 1025–1035 (2004).
23. X. Y. He, Z. B. Liu, D. N. Wang, M. W. Yang, T. Y. Hu, and J. G. Tian, "Saturable absorber based on graphene-covered-microfiber," *IEEE Photon. Technol. Lett.* **25**(14), 1392–1394 (2013).
24. Q. Sheng, M. Feng, W. Xin, T. Han, Y. Liu, Z. Liu, and J. Tian, "Actively manipulation of operation states in passively pulsed fiber lasers by using graphene saturable absorber on microfiber," *Opt. Express* **21**(12), 14859–14866 (2013).
25. M. Lotya, P. J. King, U. Khan, S. De, and J. N. Coleman, "High-concentration, surfactant-stabilized graphene dispersions," *ACS Nano* **4**(6), 3155–3162 (2010).
26. L. M. Tong, F. Zi, X. Guo, and J. Y. Lou, "Optical microfibers and nanofibers: A tutorial," *Opt. Commun.* **285**(23), 4641–4647 (2012).
27. J. N. Coleman, "Liquid exfoliation of defect-free graphene," *Acc. Chem. Res.* **46**(1), 14–22 (2013).
28. S. Kumar, M. Anija, N. Kamaraju, K. S. Vasu, K. S. Subrahmanyam, A. K. Sood, and C. N. R. Rao, "Femtosecond carrier dynamics and saturable absorption in graphene suspensions," *Appl. Phys. Lett.* **95**(19), 191911 (2009).

1. Introduction

As one-atomic-layer carbon material, graphene exhibits a variety of novel electronic and optical properties [1–3], which have inspired a variety of novel optical applications including mode-locked ultrafast lasers [4–6], optical modulators [7–9] and photodetectors [10–14]. Especially, the relaxation time of carriers in graphene is a few picoseconds [15], dominated by carrier-phonon scattering, which offers great opportunities for ultrafast light manipulation. Also, being atomically thin, graphene can be integrated with optical waveguides for enhanced light-graphene interaction [7–9,13,14,16–18]. Recently, by integrating graphene with microscale optical waveguides or microfibers, graphene photodetectors [11–14] and optical modulators [7,8] with fast response time have been demonstrated. Usually, the fabrication of these graphene-functionalized structures require complicated and time-costing graphene transfer processes. Also, the precision of spatially positioning and localization of the graphene is limited, although it is highly desired for optical functionality.

In 2009, Yamashita et al. demonstrated an evanescent field deposition method to transfer carbon nanotubes onto the sidewall of a microfiber by optical gradient force [19], which has been applied to realize mode-locked fiber lasers [19–21]. In this paper, we adopted this method to develop a graphene-decorated-microfiber (GDM) for ultrafast light modulation. Rather than microfibers with relatively large diameters (e.g., 5 μm) used in previous reports [19–21], here we use microfibers with smaller diameter (e.g., $\sim 1 \mu\text{m}$) for enhancing the light-graphene interaction, as well as for single-mode operation of the microfiber around 1550-nm wavelength (C-band of optical communication) [22]. The significantly enhanced interaction of evanescent fields and graphene flakes (overlapping on the surface of the microfiber), leads to a linear absorption as high as $\sim 1.3 \text{ dB}/\mu\text{m}$ at 1.5- μm wavelength. The measured threshold of saturable absorption is about 1.75 W in peak power, which is one order of magnitude lower than those of previous reports in similar structures [8, 23, 24]. Also, we demonstrated a transmission modulation for 1550-nm-wavelength signal using 1064-nm nanosecond laser pulses, with measured response time of 3.5 ps.

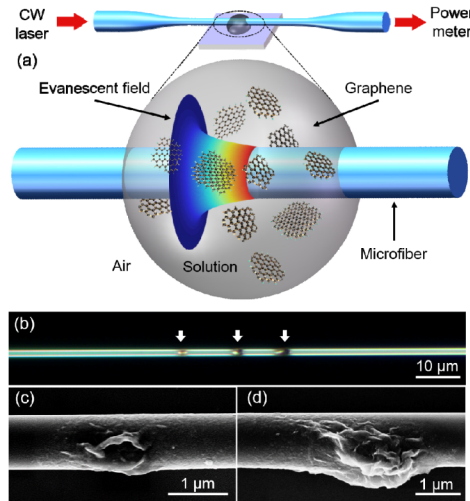


Fig. 1. Fabrication of graphene decorated microfibers (GDMs). (a) Schematic diagram of the evanescent field deposition method for trapping graphene flakes onto the sidewall of a microfiber. (b) Optical microscope image of a 1- μm -diameter microfiber decorated with three piles of graphene flakes, marked with white arrows. (c, d) Typical SEM images of GDMs fabricated with relatively short (c) and long (d) deposition time.

2. Fabrication of GDMs

The water-soluble graphene flakes, with lateral dimensions of a few hundred nanometers to several micrometers, were synthesized using a liquid-phase exfoliation method [25], and prepared as an aqueous solution. The microfibers used here, were fabricated by flame-heated taper drawing standard fibers into biconical tapers with waist sizes down to $\sim 1\ \mu\text{m}$ [26], which is thinner than those employed in previous reports [19–21]. To deposit the graphene flakes onto the surface of the 1- μm diameter microfiber, we used an optical evanescent-field deposition method [19] (as shown in Fig. 1(a)). Benefitted from the stronger evanescent field outside the microfiber, here the optical power required to trap and collect the graphene flakes can be reduced to 100 μW level, which was two orders of magnitudes lower compared with tens of milliwatts in previous reports [19, 20], and was helpful to avoid thermal damage. Instead of liquid polymer or polymer/aqueous mixture [19–21], here we used pure water with lower viscosity as the dispersant, which may also accelerate the deposition process. The insertion loss, especially the scattering from the water-air interface and the absorption of the deposited graphene during the depositing process, could also influence the laser power required for optical deposition. The amount of the deposited graphene can be estimated by monitoring the transmittance of the GDM in real time. Depends on the time of deposition, the graphene coating can be confined to a size down to $\sim 1\ \mu\text{m}$, which provides much higher precision of spatially positioning and localization of graphene compared with those obtained by complicated graphene transfer processes [8, 24]. Figure 1(b) shows three piles of graphene flakes with increasing deposition time (from left to right). The increasing darkness and the micrometer scale separation between the neighboring piles indicate the capability of precisely controlling both the amount and position of the deposited graphene. For reference, Figs. 1(c) and 1(d) show SEM images of GDMs fabricated with relatively short and long deposition time. The precision of position of the deposited graphene can be further improved by using a high-precision translation stage instead of manual operation.

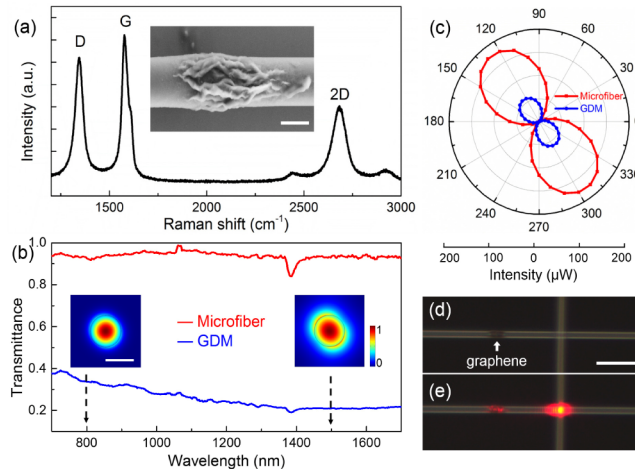


Fig. 2. Optical characterization of the GDM. (a) Raman spectrum of a graphene decorated on a microfiber. The inset was a typical SEM image of a GDM. Scale bar: 1 μm . (b) Red line and blue line were the transmittance of a pure microfiber and a GDM, respectively. Insets were cross-sectional intensity distribution of 800-nm and 1500-nm wavelength light guiding in a 1.1- μm diameter microfiber. Scale bar: 1 μm . (c) Polarization dependent optical power measured before (red line) and after (blue line) graphene deposition process. (d, e) A 1- μm -diameter GDM with a 1- μm -diameter microfiber placed across, before (d) and after (e) a 640-nm light was guided through. Scale bar: 10 μm .

3. Optical characterization of GDMs

The Raman spectrum of the graphene-coated-area of a typical GDM is presented in Fig. 2(a). The strong D peak is induced by the massive edges of small graphene flakes (see inset of Fig. 2(a)) [25, 27]. To measure the optical transmittance of a GDM with one graphene pile, we launched a supercontinuum broadband light into a 1- μm -diameter GDM with graphene cladding length of 5 μm . The light power was kept below 5 μW , far below the threshold of saturable absorption of graphene. The normalized transmittance of the GDM is shown in Fig. 2(b). For comparison, the transmittance of a pure microfiber is also provided. Within the spectral range of 700–1700 nm, the pure microfiber has nearly constant transmittance (except the water absorption peak around 1400 nm), while the GDM shows an absorption increasing with increasing wavelength, which can be explained by the stronger evanescent field around the graphene interface at longer wavelength (see insets of Fig. 2(b)). The transmittance of the GDM at 1550 nm is 22%, corresponding to a linear absorption coefficient of 1.3 dB/ μm , which is much higher than those of many other hybrid graphene/microfiber structures [8, 18, 24]. The strong linear absorption coefficient can be explained by the enhanced light-graphene interaction and the accumulating effect of the piled up graphene flakes. The asymmetric distribution of graphene around the microfiber (as shown in Fig. 1(c) and 1(d)) may induce polarization-dependent absorption characteristics. To investigate this, we measured the polarization properties of the output light before and after the graphene deposition process using a 1550-nm-wavelength linear-polarized light. The results shown that there was no obvious change of the polarization angle, but the degree of polarization decreased from 99.3% to 97.1% (as shown in Fig. 2(c)). Figures 2(d) and 2(e) show optical microscope images of a 1- μm -diameter GDM before and after guiding a 640-nm light, respectively. For intercepting the guided light, another 1- μm -diameter microfiber is placed cross the horizontal GDM. The scattering intensity of the graphene pile is much lower than that of the cross point, indicating that the insertion loss induced by the graphene scattering was much lower compared with the graphene absorption (on the same level of the transmitted light).

4. Saturable absorption of GDMs

To investigate the saturable absorption properties, we sent 1550-nm femtosecond laser pulses (83 MHz, 200 fs) into a 1.1- μm -diameter GDM and measured the dependence of transmission on the input power. As shown in Fig. 3(a), the transmittance approximately kept a constant of 16% (mainly originated from the linear absorption) until the input power reached 30 μW , and increased evidently afterward due to the saturable absorption. The measured threshold of saturable absorption is about 30 μW , corresponding to a peak power of 1.75 W and a peak power density of 60 MW/cm^2 at the surface of the microfiber, as calculated in Figs. 3(b) and 3(c). Figure 3(b) shows the calculated power density distribution on the cross-section plane of a 1.1- μm -diameter microfiber guiding a 30- μW 1550-nm-wavelength light, with radial power density (along the dotted line) depicted in Fig. 3(c). Benefitting from the enhanced light-graphene interaction and the accumulative effect of the heaped up graphene flakes, the threshold observed here (1.75 W) is one order of magnitude less than that previously reported (40.6 W) [8]. When the input power exceeded 500 μW , the graphene flakes began to be burnt away, and the transmission measurement is no longer reversible.

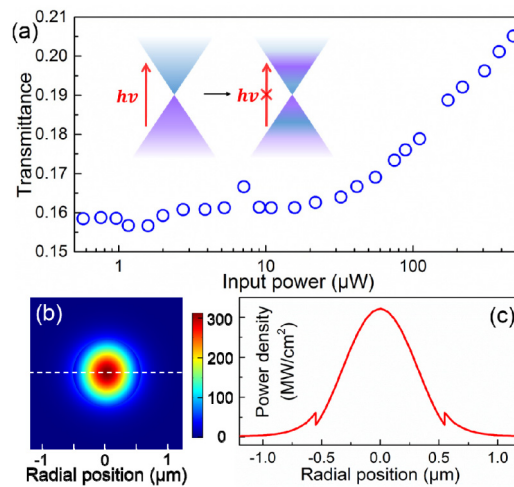


Fig. 3. Saturable absorption of a GDM. (a) Power dependent transmittance of a GDM measured with 1550 nm laser pulse (~ 200 fs, 83 MHz). Inset was the schematic diagram of saturable absorption. (b) Cross-sectional peak power distribution of the 1550-nm-wavelength light guiding in a 1.1- μm microfiber normalized to the power threshold of saturable absorption of 30 μW . (c) Power density dependence along the dotted line in (b) on the radial position.

5. Ultrafast light manipulation with GDMs

For optical modulation, we used a saturable absorption based all-optical scheme that has been reported elsewhere [8, 17]. Here 1064-nm nanosecond pulses (8 ns, 2.4 kHz) was used as switch light to turn on a 1550-nm CW light (the signal light). The switch and signal lights were coupled into standard optical fibers, combined to co-propagation beams and sent into the GDM. After guiding through the GDM, the output light passed through a longpass filter to filter out the switch light. The power of the signal light was kept a constant of 5 μW . When the average power of switch light increased to 10 μW , the switched signal was clearly observed in the output (red line shown in Fig. 4(a)). With 10- μW switch light on, when the signal light was turned off, the output signal disappeared (black background in Fig. 4(a)), confirming that the switched signal was originated from the modulated signal light. Benefitted from the highly localized graphene pile deposited on the surface of the microfiber, it is also possible to realize the cross modulation by intersecting two microfibers around the graphene pile. As shown in Fig. 4(b), modulated output was observed in a 1- μm -diameter microfiber (guiding a CW 1550-nm signal light) when a second 0.4- μm -diameter microfiber

guiding switch light (1064-nm nanosecond pulses) was perpendicularly placed on the first microfiber at the area of deposited graphene. Compared with that in the co-propagation scheme shown in Fig. 4(a), the cross modulation depth is much lower due to the much shorter overlap of the signal and the switch light on the graphene coating, which can be improved by optimizing the thickness of the graphene pile and the diameter of the microfiber. Specifically, the fractional evanescent field around the microfiber increases with decreasing diameter, which is helpful for enhancing the light-graphene interaction, and also the modulation depth. But at the same time, the insertion loss caused by the graphene absorption is inevitable, which is a balance/price for the ultra-broadband operation, and there has to be a tradeoff between the modulation depth and the insertion loss.

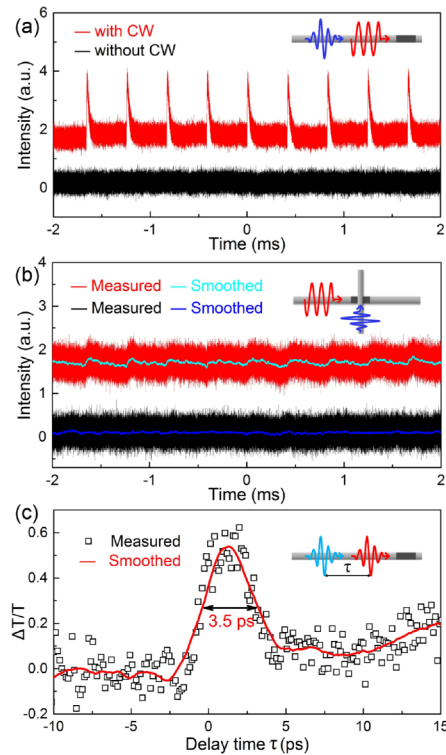


Fig. 4. Optical modulation based on GDMs. Signals (red curve) switched out from a 1550-nm CW beam in a 1- μ m-diameter GDM by a 8-ns 1064-nm switch pulse train, which was applied by (a) co-propagating in the same GDM and (b) perpendicularly propagating in a 0.4- μ m-diameter microfiber (see insets), respectively. For reference, signal output with switch on and signal off is also provided (black curve). (c) Differential transmittance of the probe light (1550 nm, 35 fs duration time) through a 1.2- μ m-diameter GDM as a function of the pump-probe time delay with pump light of 789-nm wavelength and 500-fs duration time, showing a response time of \sim 3.5 ps. Insets of (a-c) are the schematic diagrams of the modulation setups.

To explore the ultrafast response of the GDM, we used a pump-probe measurement that has been reported elsewhere [8]. The pump (789 nm wavelength, 35 fs duration) and probe (1550-nm wavelength, 500 fs duration) beams were from a same femtoseconds Ti:sapphire laser and were coupled into and co-propagated through the GDM. The pump light was filtered out at the output by a notch filter. Figure 4(c) shows the time resolved result, with fitted full width at half maximum of 3.5 ps (as red line shown), which agrees well with the previous results measured in liquid-phase exfoliated graphene flakes [28].

6. Conclusion

In summary, we have fabricated GDMs using a convenient and controllable evanescent-field-induced deposition method with fiber diameters down to 1 μm . Benefitting from the significantly enhanced light-graphene interaction in these subwavelength microfibers and accumulation of the saturable absorption of the piled graphene flakes, the microfiber shows a linear absorption coefficient as high as 1.3 dB/ μm at 1550-nm wavelength, and a nonlinear saturable absorption with peak-power threshold down to 1.75 W (60 MW/cm²). As an example for ultrafast light manipulation, we further demonstrated all-optical modulation of a 1550-nm-wavelength signal in a 1- μm -diameter GDM, with a measured response time of about 3.5 ps. The highly localized graphene deposition, very low threshold for saturable absorption, easy fabrication, compact footprint and excellent fiber compatibility of the GDM demonstrated here, may open new opportunities for ultrafast light manipulation for applications such as all-optical logical circuits and chip-integrated mode-locked lasers.

Acknowledgments

The authors thank Xin Guo, Yipei Wang, Yue Cao, Xinhai Zou and Pan Cao for their helpful discussion in sample preparation, characterization and manuscript preparation. This work was supported by the National Key Basic Research Program of China (2013CB328703) and National Natural Science Foundation of China (61475140).